Eur Respir J, 1996, 9, 93–99
DOI: 10.1183/09031936.96.09010093
Printed in UK - all rights reserved

European Respiratory Journal
ISSN 0903 - 1936

Differential role of actin in lung endothelial and epithelial barrier properties in perfused rabbit lungs

L. Ermert*+, R. Rössig*, T. Hansen*, H. Schütte*, K. Aktories**, W. Seeger*

Differential role of actin in lung endothelial and epithelial barrier properties in perfused rabbit lungs. L. Ermert, R. Rössig, T. Hansen, H. Schütte, K. Aktories, W. Seeger. ©ERS Journals Ltd 1996.

ABSTRACT: Lung fluid balance is critically dependent on capillary endothelial and alveolar epithelial barrier properties, and cytoskeletal components have been implicated in these barrier functions. In an earlier study, we perfused *Clostridium botulinum* C_2 toxin, which effects selective loss of non-muscle F-actin, through isolated rabbit lungs: a severalfold increase in the capillary filtration coefficient (*K*fc) was noted, together with attenuations and disruptions of endothelial cells upon electron microscopic examination. In this model we have investigated the influence of the C_2 toxin on alveolar epithelial barrier properties. Epithelial permeability was assessed by continuous monitoring of the transepithelial passage of technetium-labelled diethylenetriamine penta-acetic acid (^{99m}Tc-DTPA), offered to the alveolar surface by aerosol technique.

Intravascular administration of hydrogen peroxide, used as control agent, was shown to provoke a four- to fivefold increase in the clearance rate of ^{99m}Tc-DTPA under conditions of severe fluid leakage into the lung interstitial and alveolar space. Intravascular administration of C_2 toxin caused a dose- and time-dependent increase in *K*fc values (8–15 fold), but the Tc-DTPA clearance rate was entirely unaffected. Moreover, transbronchial application of C_2 toxin again reproduced the manifold increase in *K*fc data (about six fold), but the rate of transepithelial passage of the hydrophilic Tc-DTPA complex remained unchanged.

We conclude that the barrier properties of the lung microvascular endothelial and epithelial layer are differentially regulated. It is suggested that the actin microfilament system plays a decisive role in the structural and functional integrity of the endothelial but not the epithelial barrier.

Eur Respir J., 1996, 9, 93–99.

*Dept of Internal Medicine and +Institute of Anatomy and Cytobiology, Justus-Liebig University Giessen, Giessen, Germany. **Institute of Pharmacology and Toxicology, University of the Saarland, Homburg, Germany.

Correspondence: W. Seeger
Justus Liebig University Giessen
Dept of Internal Medicine
Klinikstrasse 36
D-35385 Giessen
Germany

Keywords: Botulinum C_2 toxin
endothelial permeability
epithelial permeability
isolated rabbit lung

Received: December 28 1994
Accepted after revision August 15 1995

This work was supported by the Deutsche Forschungsgemeinschaft (SFB 249).

Lung oedema formation may be caused by two basically different mechanisms: increased fluid filtration under conditions of elevated capillary pressure (hydrostatic oedema); and transudation of fluid due to inflammatory or toxic deterioration of capillary endothelial and/or alveolar epithelial barrier function (high permeability pulmonary oedema) [1, 2]. A combination of both mechanisms may also exist. Recent studies into the ultrastructural damage of the gas exchange area in rabbit lungs after exposure to high capillary pressures revealed disruptions of both endothelial and epithelial layers in variable association with additional rupture of the basement membrane [3–8]. These barrier lesions have been attributed to stress failure. The mechanisms maintaining cellular integrity and anchorage of cell-cell and cell-matrix contacts are overridden by the mechanical forces. Major importance for the maintenance of the endothelial and epithelial barrier function is attributed to the cytoskeleton, in particular actin filament stress fibres [9–11].

Interestingly, alterations reminiscent of stress failure lesions were recently noted in response to intravascular challenge of rabbit lungs with *Clostridium botulinum* C_2 toxin at low capillary pressures [12]. C_2 is a binary toxin, consisting of the two components C_{2I} and C_{2II} [13]. C_{2II} (Mr 100,000) promotes the translocation of component I into eukaryotic cells. C_{2I} (Mr 50,000) selectively adenosine diphosphate (ADP)-ribosylates non-muscle G-actin at arginine 177 [13, 14]. The covalent G-actin modification leads to a drastic inhibition of G-actin polymerization [13], and inhibits nucleation of polymerization by the gelsolin-actin complex [15]. In addition, G-actin is converted into a capping protein, which binds to the barbed end of actin filaments and, thereby, inhibits the polymerization at this site, whereas the depolymerization at the pointed end is not affected. The net effect is the progressive and virtually complete decay of F-actin [14]. In C_2 toxin-treated perfused rabbit lungs, a severalfold increase in the capillary filtration coefficient (*K*fc) was noted, accompanied by extensive oedema formation, and electron microscopic examination of these lungs revealed attenuations and disruptions of endothelial cells [12]. C_2 toxin effects were partly antagonized by the F-actin stabilizing agent phallacidin. These findings

strongly support an important role of the actin microfilament system for the structural and functional integrity of the lung capillary endothelial layer at physiological vascular pressures.

The present study was undertaken to probe the role of the actin-based filamentous network for the alveolar epithelial barrier function in intact rabbit lungs. Continuous monitoring of the transepithelial passage of aerosolized ^{99m}technetium-labelled diethylenetriamine penta-acetic acid (^{99m}Tc-DTPA) MW 492 Da was used for assessment of these barrier properties, and botulinum C_2 toxin - offered to both the endothelial and epithelial surface - was again employed for selective perturbation of actin. Both methods of toxin delivery again provoked capillary endothelial leakage, whereas the transepithelial tracer passage remained entirely unaffected. These results suggest a differential role of the actin microfilament system in capillary endothelial and alveolar epithelial barrier properties in intact lungs.

Methods

Reagents

Hydroxyethylamylopectin (MW 200,000) was received from Fresenius AG (Oberursel, Germany), $CaNa_3$-DTPA/$SnCl_2$-2 H_2O from Amersham Buchler (Braunschweig, Germany), and $^{99m}TcO_4^-$ was graciously supplied by G.L. Fängewisch, Dept of Nuclear Medicine, Giessen. All other chemicals were obtained from Merck (Darmstadt, Germany).

Preparation of C_2 toxin

Preparation of the components I and II of the toxin was performed essentially as described previously [16]. Aliquots of one batch of each toxin component, dissolved in saline, were stored at -20°C and used throughout the study. Mixing of the components was performed directly before experimental use. Saline served as control substance for sham injections.

Isolated lung model

The model has been described previously [17]. Briefly, rabbits of either sex (body weight (BW) 2.2–2.6 kg) were deeply anaesthetized and anticoagulated with heparin, 1,000 U·kg^{-1} BW. The lungs were removed with trachea and bronchi attached, whilst being perfused with Krebs-Henseleit buffer through cannulae in the pulmonary artery and the left atrium. The buffer contained 132.8 mM NaCl, 4.3 mM KCl, 1.1 mM KH_2PO_4, 24.1 mM $NaHCO_3$, 2.4 mM $CaCl_2$ and 1.3 mM $MgPO_4$, as well as 240 mg glucose and 5 g hydroxyethylamylopectin (as oncotic agent) per 100 mL. The lungs were placed in a temperature-equilibrated housing chamber at 37°C, freely suspended from a force transducer. They were ventilated *via* the trachea with 4% CO_2, 17% O_2 and N_2 (tidal volume 30 mL; frequency 30 ventilations·min^{-1}; end-expiratory pressure 1 cmH_2O), the pH of the perfusion fluid ranged 7.35–7.45. After extensive rinsing of the vascular bed, the lungs were perfused with a pulsatile flow of 150 mL·min^{-1}. Perfusion fluid was recirculated but the alternate use of two separate perfusion circuits, each containing 200 mL, allowed exchange of perfusion fluid. Perfusion pressure, ventilation pressure and the weight of the isolated organ were registered continuously. The left atrial pressure was set to 2 mmHg under baseline conditions (0 referenced at the hilum) to guarantee zone III conditions at end-expiration throughout the lung. The capillary filtration coefficient (*K*fc, given in cm^3·s^{-1}·mmHg^{-1}·g^{-1} wet lung weight ×10^{-4}) and the total vascular compliance were determined gravimetrically from the slope induced by a 7.5 mmHg step elevation of the venous pressure for 8 min. The application of this method to the present model and the use of zero time extrapolation of the slope of weight gain for the calculation of *K*fc have been described previously [17]. In lungs already displaying toxin-induced weight gain before onset of the hydrostatic challenge, the pressure step-induced rate of weight gain was corrected for this baseline rate of weight gain. In addition, the hydrostatic challenge-induced net increase in lung weight (ΔW, determined as the difference between prechallenge and 2 min post-challenge weight) was assessed. Lungs selected for the study were those that: 1) had a homogenous white appearance without signs of haemostasis or oedema formation; 2) had pulmonary artery and ventilation pressure in the normal range; and 3) were isogravimetric during a steady-state period of 40 min.

Measurement of clearance rate of inhaled aerosolized ^{99m}Tc-DTPA

The clearance rate of aerosolized ^{99m}Tc-DTPA from the lungs into the perfusion fluid was used as an index of pulmonary epithelial permeability [18–20].

Aerosol preparation and evaluation. $CaNa_3$-DTPA, 1.2 mg, and $SnCl_2$-2H_2O, 0.016 mg, were added to 0.5 mL of sterile saline in a reaction vial, followed by 270 µCi of $^{99m}TcO_4^-$ in 0.5 mL of saline, incubated for 20 min. This solution was placed in a Savac nebulizer, driven with the same gas mixture as used for lung ventilation, at a pressure of 12 Psi. To minimize dissociation of the ^{99m}Tc-DTPA complex, the radiopharmaceutical was prepared within 20 min of use. Repetitive analysis of the degree of binding between ^{99m}Tc and DTPA was performed by paper chromatography in samples collected from the residual fluid in the nebulizer and collected from the lung perfusion circuit up to 120 min after aerosol administration. Chromatography was performed in duplicate on strips 1.0×10 cm of Whatman No. 3 paper as described previously [21]; the binding surpassed 99% in all cases. Size of the aerosol particles was determined by a differential mobility analyser (DMA), connected to a condensation nucleus counter (CNC) (kindly performed by J. Gebhart, GSF, Frankfurt, Germany). The mass median aerodynamic diameter (MMAD) of the particles

was 1.1 µM, with a geometric standard deviation (GSD) of 2.1. The aerosol was delivered to the inspiration loop of the ventilator by use of a bag-in-box system; approximately 4–5 µCi ^{99m}Tc were deposited in the lung bronchoalveolar compartment within 6–10 min by use of this technique.

Data collection and calculation of clearance rate. Two 2 inch sodium-iodide detectors, connected with a Ramona G gamma counter (Raytest, Straubenhardt, Germany), were levelled to the costal side of the left lung at a distance of 3 cm to the tracheal bifurcation and to the perfusion circuit reservoir [22]. Lung and perfusate reservoir were shielded by lead from each other and from background activity. This equipment summed the number of counts every second; averaging was performed every 30 s. Absolute counts were corrected for the radioactive half-life of ^{99m}Tc (360 min) and for the difference in recoveries of tracer between lung and perfusate sampling position. The latter were assessed by separating the lung and the perfusion circuit and independently loading both with known quantities of tracer. Correction for perfusate-associated radioactivity contained in the lung vascular volume (~3 ml) was not undertaken, as this never surpassed 0.5% of total lung radioactivity (due to the large perfusate reservoir into which the tracer was diluted after transepithelial passage). Kinetics of lung and perfusate radioactivity were displayed, and the ^{99m}Tc-DTPA clearance rate was calculated as fractional decrease of lung-associated radioactivity per min (-%·min^{-1}).

Experimental design

After termination of the initial steady-state period, the recirculating Krebs-Henseleit hydroxyethylamylopectin buffer was exchanged with fresh buffer medium, preloading of the lungs with ^{99m}Tc-DTPA was performed and baseline clearance rate was measured for a 15 min period (range -0.4 to -1.6% in all experiments). Next, time was set to zero and C_2 toxin, H_2O_2 or sham challenge was undertaken. Toxin doses were chosen according to dosage used in the preceding study with intravascular application of C_2 toxin in isolated rabbit lungs [12]. Whilst radioactivity was monitored continuously, hydrostatic challenges for assessment of *K*fc were performed 20, 50 and 80 min after application of stimulus. Perfusion was terminated 2 min after finishing the third venous pressure elevation, or when the toxin-induced increase in lung weight gain (ΔW) surpassed 30 g. Six experimental groups were studied, each with five isolated lungs: *Control*. Sham application of 500 µl saline, either injected into the pulmonary artery (n=2) or applied intratracheally (n=3).

C_2 0.06/0.12 µg infus. C_{2I} (0.06 µg) and C_{2II} (0.12 µg) were premixed in 500 µL saline and infused into the pulmonary artery within 2 min.

C_2 1/2 µg infus. C_{2I} (1 µg) and C_{2II} (2 µg) were premixed in 500 µL saline and infused into the pulmonary artery within 2 min.

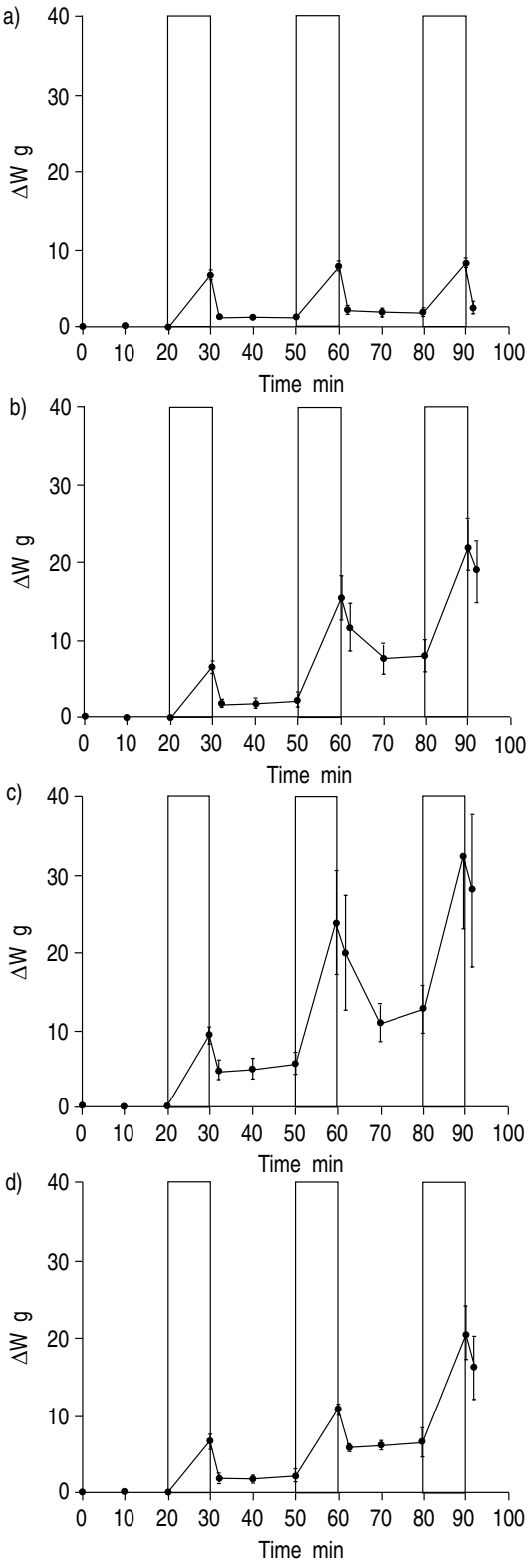

Fig. 1. – Time-course of lung weight gain (ΔW): a) in control lungs; and b–d) in lungs exposed to different C_2 toxin doses (b) C_2 1/2 µg intravascular infusion; c) C_2 2/4 µg intravascular infusion; d) C_2 2/4 µg *via* trachea). The 10 min hydrostatic challenges (20, 50 and 80 min) are indicated by columns. Mean values±SEM of five experiments each are depicted (SEM bars are missing when falling into symbol). Except for the low-dose toxin group (0.06/0.12 µg; not depicted as not differing from the control group), all groups with botulinum C_2 toxin application were significantly different from the control group.

C_2 2/4 µg infus. C_{2I} (2 µg) and C_{2II} (4 µg) were premixed in 500 µL saline and infused into the pulmonary artery within 2 min.

C_2 2/4 µg trach. C_{2I} (2 µg) and C_{2II} (4 µg) were premixed in 500 µL saline and slowly injected into the trachea *via* a small catheter whilst rotating the lung.

H_2O_2. This agent was admixed to the recirculating buffer fluid at a final concentration of 250 µM. In order to avoid a large increase in pulmonary artery pressure, the application of H_2O_2 was performed in the presence of 500 µM acetylsalicylic acid.

Statistics

All values are given as mean±SEM. For assessment of statistical significance, two-way analysis of variance was performed; significance was assumed when the p-value was less than 0.05.

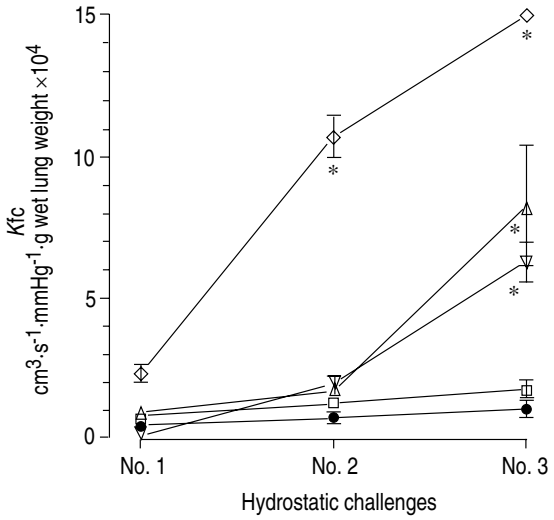

Fig. 2. – Time- and dose-dependent increase in the capillary filtration coefficient (*K*fc) in response to botulinum C_2 toxin stimulation. Hydrostatic challenges were performed 20 min (No. 1), 50 min (No. 2) and 80 min (No. 3) after toxin application. Mean values±SEM of five experiments each are depicted (SEM bars are missing when falling into symbol). After 80 min (challenge No. 3) all groups with botulinium C_2 toxin application differed significantly from the control group, except for the low-dose toxin group (0.06/0.12 µg. *: $p<0.05$. —◇—: C_2 2/4 µg infus.; —Δ— : C_2 1/2 µg infus.; —▽— : C_2 2/4 µg trach.; —□— : C_2 0.06/0.12 µg infus. —●—: control.

Results

Pulmonary artery pressure

In all lungs, the pulmonary artery pressure ranged 5–8 mmHg during the initial baseline period. In all groups vascular compliance did not change. Neither intravascular nor intratracheal challenge with botulinum C_2 toxin provoked any change in vascular perfusion pressure throughout the experiments. Due to the presence of acetylsalicylic acid, the H_2O_2-provoked increase in pulmonary artery pressure (which is known to be largely thromboxane mediated in rabbit lungs [23]) was restricted to <3 mmHg.

Endothelial permeability and lung weight gain

In control lungs and in lungs subjected to the low C_2 toxin dose of 0.06/0.12 µg, no spontaneous weight gain occurred (fig. 1), and the *K*fc values never surpassed 2.5 $cm^3 \cdot s^{-1} \cdot mmHg^{-1} \cdot g$ wet lung weight $\times 10^{-4}$ (fig. 2). The hydrostatic challenge-induced weight gain was largely reversible after termination of the manoeuvres of venous pressure elevation (fig. 1). In contrast, application of the combined components of botulinum C_2 toxin at higher dosage (1/2 and 2/4 µg infused into the circulation) caused a time- and dose-dependent, pronounced increase in *K*fc values (fig. 2). For the second challenge, lungs treated with 2/4 µg C_2 toxin differed significantly ($p<0.005$) from control lungs. For the third challenge all groups with C_2 toxin, except for the low-dose toxin group (0.06/0.12), dif-

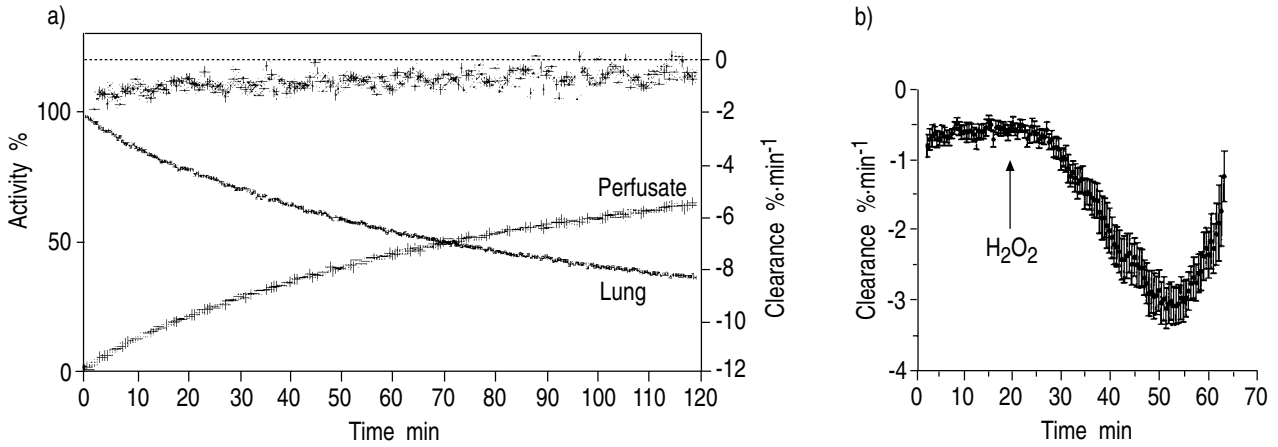

Fig. 3. – Time-course of lung ^{99m}technetium-labelled diethylenetriamine penta-acetic acid (^{99m}Tc-DTPA) clearance: a) in control lungs; and b) in lungs exposed to H_2O_2 (250 µm). a) After termination of lung ^{99m}Tc-DTPA deposition, radioactivity tracing was started over the lung (set 100%) and over the perfusate reservoir (starting point 0%) (mean values of two separate experiments shown). Counts were corrected for the different recoveries of the two tracing positions and for the decay of label. Clearance rates (-%·min^{-1}) were calculated from the decline in lung radioactivity every 30 s. The constancy of clearance rates in the two control lungs is evident. ∗: clearance rates; ■ : lung; +: perfusate. b) Marked increase in the ^{99m}Tc-DTPA clearance rate in lungs exposed to H_2O_2 (250 µm) challenge (n=5 experiments; mean±SEM bars given for each time-point).

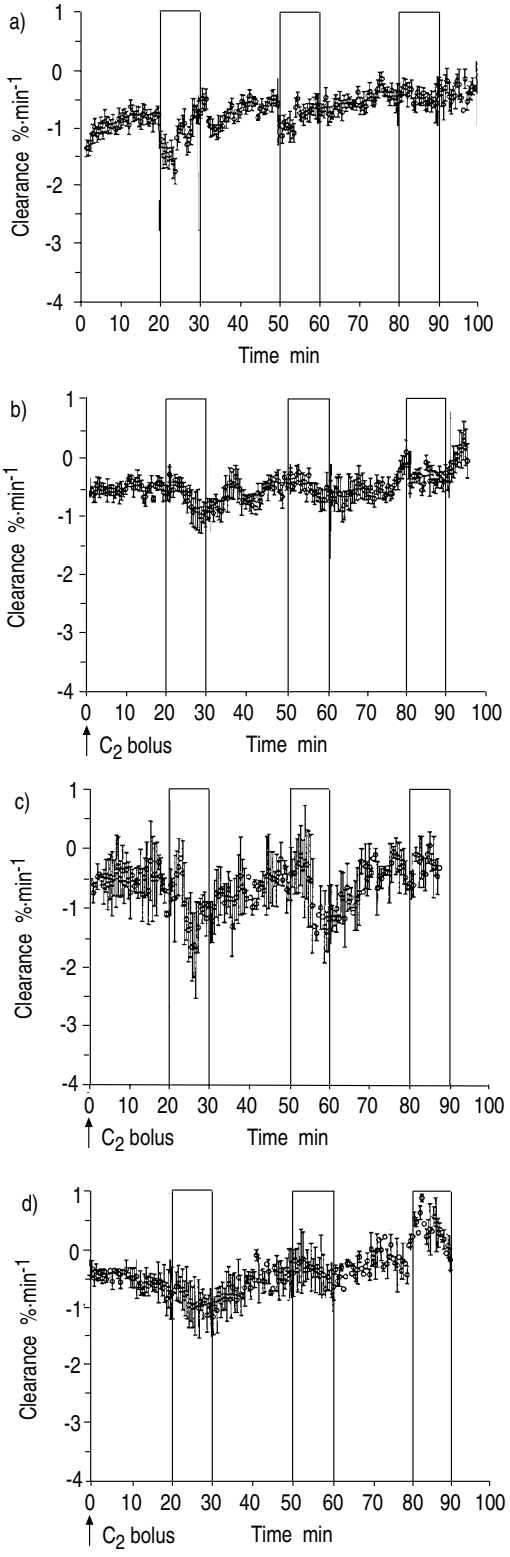

Fig. 4. – Time-course of lung ^{99m}technetium-labelled diethylenetriamine penta-acetic acid (^{99m}Tc-DTPA) clearance: a) in control lungs (n=5); and b–d) in lungs exposed to different doses of botulinum $C_{2I/II}$ (n=5 each; b) C_2 1/2 µg infus.; c) C_2 2/4 µg infus.; d) C_2 2/4 µg trach.) Clearance rates were calculated every 30 s (mean±SEM bars given for each time-point). The hydrostatic challenges (at 20, 50 and 80 min) are indicated by shaded vertical bars. None of the groups with toxin application differed from the control group. infus.: infused intravascularly; trach.: applied transtracheally.

fered significantly from the control group ($p<0.05$). There was a concomittant marked lung weight gain associated with C_2 toxin (fig. 1). A corresponding severe loss of endothelial barrier function was also noted upon intratracheal administration of the botulinum toxin. Interestingly, 2/4 µg C_2 toxin applied *via* the transbronchial route virtually completely matched the extent and kinetics of *K*fc increase (>fivefold; fig. 2) and weight gain (up to 20 g; fig. 1) in response to intravascular application of 1/2 µg toxin.

Epithelial permeability

Subsequent to ^{99m}Tc-DTPA aerosol administration, a monoexponential decrease of lung-associated radioactivity, paralleled by a countercurrent increase in perfusate counts, was noted in all control lungs (figs. 3a and 4a). The calculated DTPA clearance rate ranged 0.4–1.6%·min^{-1}, in accordance with previously published data for human and rabbit lungs [19]; it did not change over the entire observation period of 90 min in all control experiments (figs. 3 and 4a). Intravascular administration of H_2O_2 provoked protracted lung oedema formation (30 g weight gain within 55–65 min in all lungs; data not given in detail); and it also provoked a rapid, severalfold increase in the ^{99m}Tc-DTPA clearance rate up to 4–5 fold values (fig. 3b). In contrast, neither intravascular nor transtracheal application of botulinum toxin evoked any significant increase in the clearance rate of ^{99m}Tc-DTPA (fig. 4). The only change was some increased scattering of values during the hydrostatic challenges in the lungs with extensive oedema formation (2/4 µg toxin applied intravascularly; fig. 4c), which did not affect the overall kinetics of transepithelial ^{99m}Tc-DTPA passage.

Discussion

In the present study, botulinum C_2 toxin was used as a tool for selective perturbation of non-muscle F-actin. The effect of botulinum C_2 toxin on endothelial cell monolayers and human neutrophils is characterized by a time- and dose-dependent increase of G-actin and a decrease of F-actin [24, 25]. The kinetics of F-actin loss was compatible with the increase in hydraulic conductivity in the endothelial cell monolayer study [24]. As reported previously, intravascular administration of this agent in the isolated lung model provoked a dose-dependent, dramatic increase in the capillary filtration coefficient, concomitant with severe lung oedema formation, both under baseline conditions and, in particular, in response to hydrostatic challenges [12].

Preloading of lung cells in the isolated perfused lung model with phallacidin, which in opposition to C_2 toxin decreases F-actin depolymerization, significantly reduced the C_2 toxin-induced increase in vascular permeability after intravascular application of C_2 toxin [12]. As the vascular pressures were entirely unaffected, being comparable in control lungs and C_2-treated lungs, and vascular compliance did not change (data not given in detail), there was no evidence for any substantial in-

crease in endothelial surface area, and the dramatic rise in *K*fc and lung weight must be fully ascribed to an increase in the hydraulic conductivity of the lung endothelial barrier. Moreover, the extent of *K*fc rise and fluid accumulation strongly suggests that the lung microvasculature represents the predominant site of toxin attack, as it is by far the leading site of lung fluid filtration [26, 27], and the presently observed severalfold increase in hydraulic conductivity is not imaginable without major involvement of this capillary filtration site. This view is fully supported by the electron microscopic examination of C_2 toxin-treated lungs, showing attenuations and disruptions of endothelial cells throughout the capillary bed [12].

In these preceding studies, no gross morphological deterioration of alveolar epithelial cells type I was noted [12], and the current study directly focused on the permeability characteristics of this barrier. We employed continuous monitoring of the transepithelial passage of ^{99m}Tc-DTPA, offered to the alveolar surface by aerosol technique, as the clearance of this hydrophilic complex is a sensitive marker of alveolar epithelial barrier function in intact lungs [18–20]. The rate-limiting step of its escape from the alveolar surface into the perfusate is the diffusion *via* interepithelial clefts, whereas the subsequent transendothelial passage is much less restricted. The constancy of the continuously calculated clearance rate of Tc-DTPA over the entire experimental period was demonstrated in control lungs.

To probe the reliability of this technique to also assess increase in epithelial permeability under conditions of severe fluid leakage into the interstitial and alveolar spaces, we employed H_2O_2 challenge as a "positive" control group. This agent is a potent inductor of a variety of second messenger events in alveolar epithelial cells, including elevation of intracellular calcium [28]; and the latter signal may be related to contractile events with intercellular gap formation, as described for endothelial monolayers [29]. In the current perfused lung model, H_2O_2 elicited a rapid, manifold increase in the Tc-DTPA clearance in the presence of lung fluid accumulation, the extent and kinetics of which were comparable to the oedema formation in the lungs with highest C_2 toxin challenge.

In contrast to H_2O_2 stimulation, intravascular administration of botulinum C_2 toxin did not provoke any rise in Tc-DTPA clearance up to the highest concentration used [12]. One possible explanation might be a compartmental effect: due to admixture to the vascular compartment, sufficiently high concentrations might reach the endothelial, but not the epithelial cells. This interpretation was, however, questioned by the previous finding that intravascular C_2 toxin application effected fusion of lamellar bodies with each other and the cell membrane in alveolar epithelial type II cells, which is compatible with loss of actin due to C_2 toxin efficacy in this cell type. To probe any compartmental effect more directly, additional studies with transbronchial application of a high dose of botulinum toxin were performed. Interestingly, a severalfold increase in *K*fc values was again provoked, with approximately half efficacy of the transbronchially-applied, as compared to the intravascularly-administered, toxin dose. Significant access from the alveolar surface to the endothelial cells must, thus, be assumed, although it is presently unknown whether this proceeds *via* interepithelial diffusion of toxin molecules or *via* some transcellular passage by virtue of the membrane-translocating efficacy of the C_{2II} component of the botulinum toxin [13, 14]. Again, however, no increase in Tc-DTPA clearance was noted in response to the botulinum C_2 toxin challenge.

These findings strongly suggest that the actin microfilament system does not play a decisive role in the structural integrity of alveolar epithelial cells, as is evidently the case in the capillary endothelial cells. The cytoskeleton is composed of three types of protein filament - actin filaments, microtubules and intermediate filaments - which are each composed of different protein subunits [30]. The morphological organization of the cytoskeletal network differs between various cell types, and characteristic architectures of specialized intercellular contacts have been reported [31–35]. Intermediate filaments were found to be particularly prominent in cells exposed to tension forces, providing resistance against mechanical stress [30, 36]. In epithelial cells, the intermediate filament system, forming an intracellular scaffold, may play a major role for cellular stability [36], with only a minor contribution of actin.

The results of the present study differ somewhat from previous investigations in ligated intestinal loops of mice, addressing the influence of intraluminally applied botulinum C_2 toxin on the epithelial barrier characteristics [37]. In these studies, a rise in loop weight was noted, and assumed to indicate increased epithelial permeability. Either intestinal epithelial cells might differ from alveolar cells with respect to the role of actin in the maintenance of barrier properties, or some transepithelial penetration of C_2 toxin with efficacy on vascular endothelial cells may underlie the findings of OHISHI *et al.* [37], in correspondence with the current observations.

In conclusion, botulinum C_2 toxin possesses strong potency to provoke deterioration of capillary endothelial barrier function in intact lungs, independent of application *via* intravascular or transbronchial route. These findings indicate an important role for the actin microfilament system in the maintenance of structural and functional integrity of lung microvascular endothelial cells under physiological conditions. Moreover, alterations of the microfilament system could be the decisive step for the development of permeability changes due to a variety of inflammatory agents. In contrast, alveolar epithelial barrier properties are not affected by either route of C_2 toxin application. These data suggest differential regulation of the permeability characteristics in these closely adjacent barriers with respect to actin. Non-actin components of the cytoskeleton appear to predominate in the alveolar epithelial cell type.

Acknowledgements: The authors are grateful to R.L. Snipes, Department of Anatomy, Giessen for linguistically

reviewing the manuscript.

References

1. Crapo JD (Editorial). New concepts in the formation of pulmonary edema. *Am Rev Respir Dis* 1993; 147: 790–792.
2. Staub NC, Taylor CR. *In*: Edema. New York, Raven Press, 1984.
3. Elliott AR, Fu Z, Tsukimoto K, Prediletto R, Mathieu-Costello O, West JB. Short-term reversibility of ultrastructural changes in pulmonary capillaries caused by stress failure. *J Appl Physiol* 1992; 73: 1150–1158.
4. Tsukimoto K, Mathieu-Costello O, Prediletto R, Elliott AR, West JB. Ultrastructural appearances of pulmonary capillaries at high transmural pressures. *J Appl Physiol* 1991; 71: 573–582.
5. West JB, Tsukimoto K, Mathieu-Costello O, Prediletto R. Stress failure in pulmonary capillaries. *J Appl Physiol* 1991; 70: 1731–1742.
6. Costello ML, Mathieu-Costello O, West JB. Stress failure of alveolar epithelial cells studied by scanning electron microscopy. *Am Rev Respir Dis* 1992; 145: 1446–1455.
7. Bachofen H, Schürch S, Michel RP, Weibel ER. Experimental hydrostatic pulmonary edema in rabbit lungs: morphology. *Am Rev Respir Dis* 1993; 147: 989–996.
8. Bachofen H, Schürch S, Weibel ER. Experimental hydrostatic pulmonary edema in rabbit lungs: barrier lesions. *Am Rev Respir Dis* 1993; 147: 997–1004.
9. Drenckhahn D, Wagner J. Stress fibers in the splenic sinus endothelium *in situ*: molecular structure, relationship to the extracellular matrix and contractility. *J Cell Biol* 1986; 102: 1738–1747.
10. Franke RP, Grafe M, Schnittler H, Seiffge D, Mittermayer C, Drenckhahn D. Induction of human vascular endothelial stress fibers by fluid shear stress. *Nature* 1984; 307: 648–649.
11. Wong AJ, Pollard TD, Herman IM. Actin filament stress fibers in vascular endothelial cells *in vivo*. *Science* 1983; 219: 867–869.
12. Ermert L, Brückner J, Walmrath D, *et al*. Role of endothelial cytoskeleton in high-permeability edema due to botulinum C_2 toxin in perfused rabbit lungs. *Am J Physiol* 1995; 268: L753–L761.
13. Aktories K, Wegner A. ADP-ribosylation of actin by Clostridial toxins. *J Cell Biol* 1989; 109: 1385–1387.
14. Wegner A, Aktories K. ADP-ribosylated actin caps the barbed ends of actin filaments. *J Biol Chem* 1988; 263: 13739–13742.
15. Wille M, Just I, Wegner A, Aktories K. ADP-ribosylation of gelsolin-actin complexes by clostridial toxins. *J Biol Chem* 1992; 267: 50–55.
16. Ohishi I, Iwasaki M, Sakaguchi G. Vascular permeability of botulinum C_2 toxin elicited by co-operation of two dissimilar protein components. *Infect Immun* 1980; 31: 890–895.
17. Seeger W, Walmrath D, Menger M, Neuhof H. Increased lung vascular permeability after arachidonic acid and hydrostatic challenge. *J Appl Physiol* 1986; 61: 1781–1789.
18. Staub NC, Hyde RW, Crandall E. Workshop on techniques to evaluate lung alveolar-microvascular injury. *Am Rev Respir Dis* 1990; 141: 1071–1077.
19. Smith RJ, Hyde RW, Waldman DL, *et al*. Effect of pattern of aerosol inhalation on clearance of technetium^{99m}-labeled diethylenetriamine penta-acetic acid from the lung of normal humans. *Am Rev Respir Dis* 1992; 145: 1109–1116.
20. Wiener-Kronisch JP, Albertine KH, Matthay MA. Differential responses of the endothelial and epithelial barriers of the lung in sheep to *Escherichia coli* endotoxin. *J Clin Invest* 1991; 88: 864–875.
21. Waldmann DL, Weber DA, Oberdoerster G. Chemical breakdown of technetium^{99m}-DTPA during nebulization. *J Nucl Med* 1987; 28: 378–382.
22. Schütte H, Rosseau S, Walmrath D, Grimminger F, Ernst Ch, Seeger W. Neutrophil passage through isolated perfused rabbit lungs. *Am J Physiol* 1991; 261: H1317–H1323.
23. Seeger W, Suttorp N, Schmidt F, Neuhof H. The glutathione redox cycle as a defense system against hydrogen peroxide-induced prostanoid formation and vasoconstriction in rabbit lungs. *Am Rev Respir Dis* 1986; 133: 1029–1036.
24. Suttorp N, Polley M, Seybold J, *et al*. Adenosine diphosphate ribosylation of G-actin by botulinum C_2 toxin increases endothelial permeability *in vitro*. *J Clin Invest* 1991; 87: 1575–1584.
25. Grimminger F, Sibelius U, Aktories K, Just I, Seeger W. Suppression of cytoskeletal rearrangement in activated human neutrophils by botulinum C_2 toxin. *J Biol Chem* 1991; 266: 19276–19282.
26. Fishman AP. Pulmonary edema. *In*: Fishman AP, eds. Pulmonary Diseases and Disorders. New York, McGraw-Hill, 1988; pp. 919–952.
27. Malik AB, Staub NC. Mechanism of lung microvascular injury. NY Acad Sci 1982.
28. Rice KL, Duane PG, Archer SL, Gilboe DP, Niewoehner DE. H_2O_2 injury causes Ca^{2+} dependent and independent hydrolysis of phosphatidylcholine in alveolar epithelial cells. *Am J Physiol* 1992; 263: L430–L438.
29. Suttorp N, Weber U, Welsch T, Schudt C. Role of phosphodiesterases in the regulation of endothelial permeability *in vitro*. *J Clin Invest* 1993; 91: 1421–1428.
30. Alberts B, Bray D, Lewis J, Raff M, Roberts K, Watson JD. *In*: Molecular Biology of the Cell. New York, Garland Publishing Inc., 1994.
31. Madara JL. Intestinal absorptive cell tight junctions are linked to cytoskeleton. *Am J Physiol* 1987; 253: C171–175.
32. Gumbiner B. Structure, biochemistry and assembly of epithelial tight junctions. *Am J Physiol* 1987; 253: C749–758.
33. Schneeberger EE, Karnovsky MJ. Substructure of intercellular junctions in freeze-fractured alveolar-capillary membranes of mouse lung. *Circ Res* 1976; 38: 404–411.
34. Schneeberger EE. Heterogeneity of tight junction morphology in extrapulmonary and intrapulmonary airways of the rat. *Anat Rec* 1980; 198: 193–208.
35. Schneeberger EE, Lynch RD. Structure, function and regulation of cellular tight junctions. *Am J Physiol* 1992; 262: L647–L661.
36. Bershadsky AD, Vasiliev JM. Cytoskeleton. New York, Plenum Publishing Corp., 1988.
37. Ohishi I. Response of mouse intestinal loop to botulinum C2 toxin: enterotoxic activity induced by co-operation of nonlinked protein components. *Infect Immun* 1983; 40: 691–695.